Published in final edited form as:
In Vivo. 2013 ; 27(5): 571–582.

Radioresistance of Bone Marrow Stromal and Hematopoietic Progenitor Cell Lines Derived from Nrf2−/− Homozygous Deletion Recombinant-Negative Mice

HEBIST BERHANE, **MICHAEL W. EPPERLY**, **SHAONAN CAO**, **JULIE P. GOFF**, **DARCY FRANICOLA**, **HONG WANG**, and **JOEL S. GREENBERGER**
Department of Radiation Oncology, University of Pittsburgh Cancer Institute, Pittsburgh, PA, U.S.A

Abstract

Aim: We determined whether bone marrow from $Nrf2^{-/-}$ compared with $Nrf2^{+/+}$ mice differed in response to the oxidative stress of continuous marrow culture, and in radiosensitivity of derived stromal and interleukin-3 (IL-3)-dependent hematopoietic progenitor cells. Materials and Methods: Hematopoiesis longevity in $Nrf2^{-/-}$ was compared with $Nrf2^{+/+}$ mice in long-term bone marrow cultures. Clonogenic irradiation survival curves were performed on derived cell lines. Total antioxidant capacity at baseline in nonirradiated cells and at 24 hours after 5 Gy and 10 Gy irradiation was quantitated using an antioxidant reductive capacity assay. Results: Long-term cultures of bone marrow from $Nrf2^{-/-}$ compared to $Nrf2^{+/+}$ mice demonstrated equivalent longevity of production of total cells and hematopoietic progenitor cells forming multi-lineage hematopoietic colonies over 26 weeks in culture. Both bone marrow stromal cell lines and Il-3-dependent hematopoietic progenitor cell lines derived from $Nrf2^{-/-}$ mouse marrow cultures were radioresistant compared to $Nrf2^{+/+}$-derived cell lines. Both DNA repair assay and total antioxidant capacity assay showed no defect in $Nrf2^{-/-}$ compared to $Nrf2^{+/+}$ stromal cells and IL-3-dependent cells. Conclusion: The absence of a functional Nrf2 gene product does not alter cellular interactions in continuous marrow culture, nor response to dsDNA damage repair and antioxidant response. However, lack of the Nrf2 gene does confer radioresistance on marrow stromal and hematopoietic cells.

Keywords

Hematopoiesis; bone marrow culture; Nrf2; bone marrow stromal cells; hematopoietic cells; interleukin-3

The redox sensitive transcriptional activating factor Nuclear factor (erythroid-derived 2)-like 2 (*Nrf2*) has been shown to be sensitive to radical oxygen species (ROS) for its induction (1-3). Furthermore, *Nrf2* responsive binding sites on promoters for inflammatory cytokines and other stress response genes have a prominent role in cellular, tissue, and organ response

Correspondence to: Joel S. Greenberger, MD, F.A.C.R.O., Claude Worthington Benedum, Professor and Chairman, University of Pittsburgh Cancer Institute, Department of Radiation Oncology, 5150 Centre Avenue, Pittsburgh, PA 15232, U.S.A. Tel: +1 4126473602, Fax: +1 4126476029, greenbergerjs@upmc.edu.

to various forms of oxidative stress, including irradiation (4-9). The cellular response to ionizing irradiation is complex and involves many molecular biological events initiated at the nucleus, communicated to the mitochondria, leading to the induction of apoptosis (10, 11). The complexity of the irradiation response also involves indirect effects between cells and tissues mediated by inflammatory cytokines, the induction of which is dependent upon both redox-sensitive and DNA repair-dependent transcriptional activators. While *Nrf2* homozygous deletion recombinant mice have a reduced lung fibrotic response following irradiation (4), the lifetime of these mice is also shortened (5). *Nrf2* has also been shown to be necessary for a successful resolution of the normal acute inflammatory response (8, 9). The data suggest that *Nrf2*-induced molecular biological downstream events may be involved in both early and the late tissue effects of irradiation (5-7).

A critical tissue in the irradiation response in which the interaction between stem cells and supportive stromal cells can be studied is the bone marrow (10). Total-body irradiated mice demonstrate many parameters of genetic control of the hematopoietic cellular response to irradiation (12). The role of *Nrf2* in hematopoiesis is a subject of interest (3). Recent data show that $Nrf2^{-/-}$ mice have an enlarged stem cell pool attributable to faster self-renewal, but leading to increasing senescence and less regulatory control (28). The interaction of *Nrf2* with the stem cell quiescence controlling factor chemokine receptor type-4 (CXCR4) has recently been reported (28). In the present studies, we used a continuous bone marrow culture system (13-19) to evaluate the effect of homozygous deletion of the *Nrf2* gene and its protein product, on the size and stability of the hematopoietic stem cell pool and the response of mouse bone marrow to oxidative stress. The high oxygen incubator system has been used to test whether mouse genotype (14), oxidative stress response elements (10), and inflammatory cytokine pathway gene products (18) influence longevity of hematopoietic stem cell maintenance *in vitro*.

We also tested the radiation sensitivity of culture-derived bone marrow stromal cells (mesenchymal stem cells) (16) and IL-3 dependent hematopoietic progenitor cell lines derived from these marrow cultures (15), compared to those from wild type $Nrf2^{+/+}$ mice.

Materials and Methods

Mice

Homologous recombinant negative $Nrf2^{-/-}$ mice and $Nrf2^{+/+}$ littermates were obtained from Dr. Thomas Kensler and Dr. Dionysios Chartoumpekis, University of Pittsburgh, Pittsburgh, PA, USA.

Mice were housed five per cage and fed standard Purina Laboratory Chow according to University of Pittsburgh Institutional Animal Care and Use Committee (IACUC) Institutional regulations.

Continuous bone marrow cultures

The methods for establishment of long-term (continuous) bone marrow cultures have been published previously (13-14). Briefly, the contents of adult mouse femurs and tibias were flushed through a 17-gauge needle into 25 cm. square plastic flasks (Corning, Corning, NY,

USA) and maintained in a high humidity incubator with 7% CO-2, in Fisher's medium supplemented with 15% heat-inactivated fetal calf serum with penicillin and streptomycin. Cultures were supplemented with 10^{-5} M hydrocortisone sodium hemisuecinate (13). Fresh corticosteroid was added weekly according to published methods (13).

Non-adherent cells were removed weekly and total cells counted, and then plated in 0.8% methylcellulose-containing medium supplemented with growth factors for hematopoiesis according to published methods (15). For described experiments, eight cultures were established from four mice (one tibia and one femur per flask) for each of the genotypes studied. Cultures were scored weekly for the percentage of surface area covered with adherent cells, number of cobblestone islands (representative of adherent hematopoietic stem cell-containing cell populations), as well as for non-adherent cells produced per flask, and number of non-adherent cells producing day 7 and day 14 colony-forming units (17-19). Day 7 and 14 granulocyte-macrophage progenitor (CFU-GM) colonies were counted by inverted microscopy at each time point as published elsewhere (10).

Data for weekly cobblestone island numbers, non-adherent cell numbers, percentage confluence of adherent cells, day 7 colony counts and day 14 colony counts were collected at week 1 through week 18. Each week, the cobblestone numbers for each mouse (collected from two flasks) were averaged. Three mice were compared in each group ($Nrf2^{-/-}$ and $Nrf2^{+/+}$) (total of six data points). The two groups were compared each week with the two-sided two-sample *t*-test, using the averaged numbers. Similar calculations were performed for non-adherent cell numbers and for the percentage confluence of adherent cells. For day 7 and day 14 colony-forming progenitor cell counts, observations were compared between the two groups each week with the two-sided two-sample *t*-test. As this was an exploratory study, *p*-values were not adjusted for multiple comparisons.

Derivation of bone marrow stromal cell lines

Adherent cells from long-term bone marrow cultures at 20 weeks were transferred by trypsinization to plastic petri dishes and grown in Dulbecco's modified Eagle's medium supplemented with 10% fetal calf serum, penicillin and streptomycin (19). Cell lines were expanded conservatively and then cloned in Poisson distribution methods according to published procedures (19). Clonal lines of $Nrf2^{-/-}$ and $Nrf2^{+/+}$ bone marrow stromal cell cultures were expanded according to published methods (17, 19).

Derivation of IL-3-dependent hematopoietic progenitor cell lines

Non-adherent cells were harvested from long-term culture of bone marrow cells from $Nrf2^{-/-}$ and $Nrf2^{+/+}$ mice at week 4 and cultured in six-well tissue culture plate with 4.0 ml of Iscoves modified Eagles medium supplemented with 20% fetal calf serum and 1.0 ng/ml of recombinant IL-3 (Peprotech, Rocky Hill, NJ, USA). The cells were passaged weekly by cytocentrifugation at 300 ×*g* and replenished with 4.0 ml medium. Cells were kept at high density and passaged weekly by this method for 10 weeks, at which time the mixture was split to two. From the passage at week 10, the cells were frozen at −80°C for one week, and thawed for culture in the same medium as described above. The re-cultured cells were

termed as primary Il-3-dependent cell lines and split for colony assay and sub-cloning (15, 16, 19-22).

Clonogenic radiation survival curves

The methods for radiation survival curves for adherent cell lines (29) and non-adherent hematopoietic progenitor cell lines (20-21) have been published previously. Briefly, cells were irradiated to doses between 0 and 800 cGy using a J. L. Shepard Mark I Cesium irradiator (JL Shepard and Associates, San Fernando, CA, USA) at 70 cGy per minute. Adherent cells were plated in quadruplicate in 4-well tissue culture plates and stained seven days later with crystal violet, and colonies of greater than or equal to 50 cells were scored at seven days. Non-adherent cells were plated in triplicate in methylcellulose containing recombinant mouse stem cell factor (Scf), Il-3, Il-6, and erythropoetin (Epo) (Stem Cell Technologies, Vancouver, BC, Canada) and CFU-GM colonies were scored on day seven. Survival curves were analyzed by linear regression and single-hit multi-targeted analysis according to published methods (21). D_0 (slope of the linear portion of the irradiation survival curve) and ñ (measurement of the shoulder on the survival curve which is calculated as the back extrapolation of the linear portion of the survival curve to the Y axis) were determined using linear quadratic and single-hit, multi-target models. The plating efficiency was determined by dividing the number of colonies per well at 0 Gy by the number of cells plated per well.

DNA repair measurements by comet assay

Measurement of DNA strand breaks after irradiation was performed as described previously (29). Cells of the *Nrf2*$^{-/-}$ and *Nrf2*$^{+/+}$ bone marrow stromal cell lines were irradiated and incubated at 37°C for 0, 10 min., 1 h, 6 h, or 24 h, at which time the cells were rapidly chilled to 4°C to stop DNA repair. The cells were mixed in low-melt agarose, and 500 cells were placed on the sample area of a CometSlide (Comet Assay 4250-050-K; Travigen, Inc., Gaithersburg, MD, USA). The slides were rapidly chilled to 4°C and kept in the dark to prevent DNA repair. The slides were then placed in prechilled lysis solution and kept at 4°C for 60 min, followed by washing in neutral electrophoresis buffer for 30 min at 4°C and electrophoresis at 21 V for 1 hour at 4°C. They were then immersed in DNA precipitation solution for 30 min at room temperature, immersed in 70% ethanol for 30 min, and dried at 45°C for 15 min. The cells were then stained with SYBR Green 1 and examined under a fluorescence microscope, and the comet tails for each of at least 150 cells were quantified using Comet Assay IV software (29).

Measurements of antioxidant stores by Trolox assay

Total antioxidant status of the adherent *Nrf2*$^{-/-}$ and *Nrf2*$^{+/+}$ cell lines was determined using an antioxidant reductive capacity assay (Northwest Life Science Specialties, Vancouver, BC, Canada) as previously published (23). Cells were assayed at 24 h after irradiation to 0, 5, or 10 Gy. Protein samples were standardized to 1 mg/ml using the Bradford protein assay. The antioxidant reductive assay measures the antioxidant capacity of cells based on the ability of cellular antioxidants to reduce Cu^{++} to Cu^{+}, which reacts with bathocuproine to form a color complex with absorbance at 480 to 490 nm. The net absorbance values were

compared to those of a standard curve and results reported as mM Trolox equivalents per mg protein (29).

Statistical analysis of cell line antioxidant levels and comet assays

The comet tail intensity was summarized by median and interquartile range (IQR) for each stromal cell or Il-3-dependent cell line and radiation dose (0 or 5 Gy) at different time (10, 20, or 30 min) after irradiation. The data distribution was skewed to the right. The two-sided Wilcoxon rank sum test was used to compare between the cell lines at different radiation doses and different times after irradiation. The data were then log-transformed so that their distribution was close to normal and a linear mixed model was built on the log-transformed data in all the 5 Gy-irradiated groups, using cell line and time of measurement, and their interaction term as fixed explanatory variables. Each experiment was considered as a random effect, therefore, a total of six experiments were carried out. The F-test in this model was used to compare slopes between the cell lines and a significant *p*-value indicates a significant different in the change of tail intensity with time after radiation.

Student's *t*-test was used to analyze statistical differences in radiation sensitivity and antioxidant levels. In all these tests, a *p*-value of less than 0.05 was regarded as significant. We did not adjust *p*-values for multiple comparisons. These analyses were carried out with SAS software (SAS Institute, Inc, Cary, NC, USA).

Results

Long-term bone marrow cultures were established by flushing the femur and tibia bone marrow from groups of four *Nrf2*$^{-/-}$ and *Nrf2*$^{+/+}$ mice using the contents of one femur and one tibia per flask, two flasks per mouse, and eight flasks per group (13, 14). Long-term marrow cultures were maintained at 37°C in a high humidity incubator according to published methods (14). The adherent layer of each marrow culture was scored for the percentage confluence using an inverted microscope and for the number of cobblestone islands, reflective of hematopoietic adherent islands, on the stromal cell layer weekly as described previously (10). Hematopoiesis was compared over the duration of generation of non-adherent cells and production by these non-adherent cells of hematopoietic progenitors capable of forming greater than 50 cell colonies in semi-solid medium was scored at day 7 or day 14 after subculture in secondary cultures (18).

Hematopoiesis in long-term cultures of bone marrow from Nrf2$^{-/-}$ mice is not diminished compared to those from wild-type Nrf2$^{+/+}$ mice

We compared several parameters of hematopoiesis in long-term cultures from *Nrf2*$^{-/-}$ compared to *Nrf2*$^{+/+}$ mice. As shown in Figure 1A, the time for cultures to reach confluence was indistinguishable between the two genotypes. The establishment of an adherent layer is associated with formation on that adherent layer of flattened hematopoietic cell islands termed cobblestone islands (13, 14, 27). As shown in Figure 1B, there was no difference in the number of cobblestone islands detected weekly in marrow cultures, nor in the cumulative number of cobblestone islands detected over multiple weeks of observation (Figure 1B and C, respectively).

These data establish that the oxidative stress of culture in a high humidity incubator did not produce a condition in which absence of the *Nrf2* gene product negatively impacted the capacity of adherent cell progenitors to proliferate and cover the surface of the tissue culture flask, in comparison to the stromal cell proliferation of marrow derived from $Nrf2^{+/+}$ mice.

Cobblestone islands in long-term marrow culture generate non-adherent cells which are released weekly into the fluid phase of the cultures (13, 14). Demi-de-population of the cell number by removing tissue culture medium and replacing it with a fresh volume of tissue culture medium is associated with harvest of non-adherent cells. As shown in Figure 1D, the weekly production of non-adherent cells from long-term marrow cultures derived from $Nrf2^{-/-}$ mice showed equivalent patterns of production of cells comparable to those of $Nrf2^{+/+}$. Cycling and production of cells is a common phenomenon in long-term bone marrow cultures and reflects varying rates of proliferation of differentiated progenitor cells derived from the cobblestone islands in the adherent layer (13-14).

The cumulative production of non-adherent cells (Figure 1E) showed no detectable difference between $Nrf2^{-/-}$ and $Nrf2^{+/+}$ long-term bone marrow cultures. Thus, the fluctuation and cycling in production of non-adherent cells is comparable between the cultures derived from the bone marrow of each of the two mouse genotypes.

Long-term bone marrow culture produced non-adherent cells with the capacity for proliferation to form colonies in semi-solid medium. Colony-forming progenitors cultured in semi-solid medium containing hematopoietic growth factors, including Il-3, granulocyte macrophage colony-stimulating factor Il-3, Il-6, Scf, and other combinations of growth factors, have been classified as those rapidly proliferating to form a 50-cell or greater colony within several days, and a slower proliferating population, more characteristic of the multi-lineage hematopoietic stem cell, which forms colonies at day 14 (17, 18).

As shown in Figure 1F, weekly production of day 7 colony-forming progenitor cells was similar between $Nrf2^{-/-}$ and $Nrf2^{+/+}$ cultures. Cumulative production of day 7 colony-forming progenitors was also indistinguishable between bone marrow cultures from mice of each of the two genotypes (Figure 1G).

At day 14, patterns of colony formation were indistinguishable between cultures from $Nrf2^{-/-}$ and $Nrf2^{+/+}$ mice (Figure 1H), and cumulative production of day 14 colony-forming progenitor cells was similar in the two cultures (Figure 1I). Therefore, in each of the metrics of health and proliferation in tissue culture of adherent bone marrow stromal cells and hematopoietic cells forming cobblestone islands, non-adherent cells, and colony-forming progenitor cells, there was no detectable difference between the biology of those cultures derived from $Nrf2^{-/-}$ compared to $Nrf2^{+/+}$ mice (Tables I-V).

Radioresistance of $Nrf2^{-/-}$ bone marrow stromal and Il-3-dependent hematopoietic progenitor cell lines

Permanent bone marrow stromal cell lines were derived from the adherent layer of week 4 long-term cultures of bone marrow from $Nrf2^{-/-}$ and $Nrf2^{+/+}$ mice using previously published methods (18). The radiobiology of cell lines was compared using the clonogenic

survival curve methods previously described (29). As shown in Figure 2A, bone marrow stromal cell lines from long-term cultures, bone marrow from *Nrf2*$^{-/-}$ mice demonstrated radioresistance by increase in both D_0 (dose required to reduce the fraction of cells to 37%) and ñ (measurement of the shoulder of the survival curve by extrapolating the slope of the survival curve to the Y axis with a larger number correlating to an larger shoulder) compared to cell lines derived from control *Nrf2*$^{+/+}$ mice. Clonogenic survival of *Nrf2*$^{-/-}$ Il-3 dependent hematopoietic progenitor cell lines also showed radioresistance by increase in both D_0 and ñ compared to cell lines derived from *Nrf2*$^{+/+}$ marrow cultures (Figure 2B).

Therefore, while there was no difference in the longevity and robustness of hematopoiesis in long-term bone marrow cultures, there was a clearly detectable difference in the clonogenic irradiation survival curves of both adherent bone marrow stromal cells and Il-3-dependent hematopoietic progenitor cells derived from *Nrf2*$^{-/-}$ compared to *Nrf2*$^{+/+}$ mice.

DNA repair measured by the comet assay

We next measured DNA repair kinetics in marrow stromal cell lines according to published methods (29). *Nrf2*$^{-/-}$ bone marrow stromal cell lines showed no differences in DNA repair by the comet assay compared to *Nrf2*$^{+/+}$ stromal cells (Figure 3). Both *Nrf2*$^{+/+}$ and *Nrf2*$^{-/-}$ stromal cells initiated DNA repair within an hour and completed repair by six hours. The lack of difference in DNA repair by comet assay suggests that the radioresistance of *Nrf2*$^{-/-}$ cells is attributable to differences in radiobiology following DNA damage such as mitochondrial membrane depolarization, increased production of reactive oxygen species (ROS) and might be related to differences in antioxidant stress relative to a mitochondrial mechanism of apoptosis or autophagy.

Antioxidant stress assay

Radioresistance of *Nrf2*$^{-/-}$ cell lines may have been attributable to differences in post-nuclear events leading to apoptosis. We next measured antioxidant stores in cell lines by Trolox assay. There was a significant decrease in baseline antioxidant levels in *Nrf2*$^{-/-}$ marrow stromal cells compared to the level in *Nrf2*$^{+/+}$ cells (p=0.0205). *Nrf2*$^{+/+}$ stromal cells exhibited depletion of antioxidant stores at 24 h after 10 Gy irradiation. The *Nrf2*$^{+/+}$ stromal cells had a significant decrease in the antioxidant stores compared to the level prior to irradiation (p=0.0035) (Figure 4A). In contrast, *Nrf2*$^{-/-}$ cells exhibited no significant decrease in antioxidant levels following 5 or 10 Gy irradiation. With Il-3 dependent cell lines, the results were similar for the *Nrf2*$^{+/+}$ stromal cells; however, *Nrf2*$^{-/-}$ Il-3-dependent cells exhibited an increase in antioxidant stores after 5 Gy and a further increase after 10 Gy irradiation (Figure 4B).

Discussion

Nrf2 is a transcriptional activator which binds to specific regions on the promoter of a wide variety of stress response genes, cytokine reactive genes, and genes involved in the cell cycle and metabolic function of cells. Furthermore, Nrf2 has been described as a proto-oncogene because of its activity in multiple pathways associated with malignant transformation (24). Activation of the *Nrf2* gene product has been shown to be sensitive to

oxidative stress and is induced by ROS leading to its designation as a ROS-sensitive promoter (3).

Based on the known functions of Nrf2 and its putative involvement in multiple cell biological pathways including malignant transformation, we tested the hypothesis that the oxidative stress of prolonged culture of bone marrow would lead to activation of Nrf2 and the downstream activation of stress response genes and cytokines associated with the ROS response. Therefore, we expected that the absence of Nrf2 in *Nrf2*$^{-/-}$ mice would lead to a detectable difference in oxidative stress response in their bone marrow stromal cells and hematopoietic stem cells, resulting in reduced longevity of hematopoiesis. A defect in oxidative stress handling has been associated with reduced longevity of hematopoietic stem cells in the adherent layer of marrow cultures (cobblestone islands), along with a reduced cumulative production of hematopoietic cells and colony-forming progenitor cells (10, 14, 17-19). We did not observe a detectable reduction in these parameters in long-term bone marrow cultures of *Nrf2*$^{-/-}$ compared to *Nrf2*$^{+/+}$ wild type C57BL/6J cells. The lack of detectable differences in production of day 14 colony forming unit-granulocyte, erythrocyte, monocyte/macrophage, megakaryocyte (CFU-GEMM), representing the most primitive colony-forming cells released by long term bone marrow cultures may be attributable to balanced effects of an increase in the hematopoietic stem cell pool of *Nrf2*$^{-/-}$ mice but more rapid senescence of those same cells (28). Alternatively, the *in vitro* culture system may have removed other factors regulating the effects of the *Nrf2*$^{-/-}$ genotype *in vivo*.

We saw no detectable indication of increase in the oxidative stress from *Nrf2*$^{-/-}$ mice. The effect of oxidative stress on the adherent bone marrow stromal cells in long-term culture has been associated with adipocyte differentiation (25) and sloughing of the adherent layer in marrow cultures associated with accumulation of lipid (13). If handling of oxidative stress were a critical component of maintaining the adherent layer in long-term bone marrow cultures and/or accumulation of lipid in stromal cells led to sloughing and deformation of the hematopoietic microenvironment, we would expect to see reduced longevity of hematopoiesis. We did not see such an effect on longevity of hematopoiesis in long-term cultures of bone marrow from *Nrf2*$^{-/-}$ compared to *Nrf2*$^{+/+}$ mice.

The interaction between bone marrow stromal and hematopoietic stem cell adherent islands (cobblestone islands) has been shown to be critically involved in the generation of most primitive hematopoietic stem cells (26, 27). If the functional association between hematopoietic and stromal cells were defective in *Nrf2*$^{-/-}$ marrow cultures, we would have expected to see a decrease in day 14 CFU-GEMM hematopoietic progenitor cells representative of the more primitive hematopoietic stem cells, compared to those scored at day 7. We also saw no evidence of a reduction in this parameter of interaction of hematopoietic and stromal cells in long-term culture.

Bone marrow stromal cell and hematopoietic stem cell radiation biology has been shown to correlate with defects in DNA repair, inability to handle oxidative stress of the exposure to ionizing irradiation, and other abnormalities in inflammatory cytokine responses (10, 18, 29). The results of radiation survival curves of *Nrf2*$^{-/-}$ compared to wild-type *Nrf2*$^{+/+}$ bone marrow stromal cells and hematopoietic stem cells showed clear radioresistance of *Nrf2*$^{-/-}$

cells, with an increase in both D_0 and ñ in *Nrf2*$^{-/-}$ cells. Thus, the oxidative stress involved in clonogenic survival of ionizing irradiation was paradoxically handled more effectively by *Nrf2*$^{-/-}$ compared to *Nrf2*$^{+/+}$ bone marrow stromal and Il-3-dependent hematopoietic cells. The radioresistance of *Nrf2*$^{-/-}$ cells was not a result of compensatory response to DNA damage repair as shown by comet assay. Since both stromal and Il-3-dependent cell lines exhibited a robust increase in levels of antioxidant stores after irradiation, we conclude that an enhanced cellular response leading to reduced apoptosis of *Nrf2*$^{-/-}$ cells occurred at the mitochondrial level.

Our results indicate that the absence of Nrf2 does not have a deleterious effect on hematopoiesis *in vitro* by altering interaction between hematopoietic stem cells with stromal cells in long term bone marrow cultures. The *Nrf2*$^{-/-}$ genotype did influence the intrinsic radiation biology as reflected in radioresistance of bone marrow stromal cell lines and Il-3-dependent hematopoietic progenitor cell lines. Thus, our results support a redundant system in the management of oxidative stress leading to normalization of continuous hematopoiesis under high oxygen incubation long term bone marrow culture and improved handling of the acute oxidative stress as a result of ionizing irradiation.

Acknowledgments

Supported by NIAID/NIH grant U19A1068021.

References

1. McDonald JT, Kim K, Norris AJ, Vlashi E, Phillips TM, Lagadec C, Donna LD, Ratikan J, Szelag H, Hlatky L, McBride WH. Ionizing radiation activates the Nrf2 antioxidant response. Cancer Res. 2010; 70:8886–8892. [PubMed: 20940400]
2. Li H, Wu S, Shi N, Lian S, Lin W. Nrf2/HO-1 pathway activation by manganese is associated with reactive oxygen species and ubiquitin-proteasome pathway, not MAPKS signaling. J Appl Toxicol. 2011; 31:690–697. [PubMed: 21384399]
3. Merchant AA, Singh A, Matsui W, Biswal S. The redox-sensitive transcription factor Nrf2 regulates murine hematopoietic stem cell survival independently of ROS levels. Blood. 2011; 118:6572–6580. [PubMed: 22039262]
4. Kikuchi N, Ishii Y, Morishima Y, Yageta Y, Haraguchi N, Itoh K, Yamamoto M, Hizawa N. Nrf2 protects against pulmonary fibrosis by regulating the lung oxidant level and Th1/Th2 balance. Respir Res. 2010; 11:31–39. [PubMed: 20298567]
5. Travis EL, Rachakonda G, Zhou X, Korhonen K, Sekhar KR, Biswas S, Freeman ML. Nrf2 deficiency reduces life span of mice administered thoracic irradiation. Free Rad Biol Med. 2011; 51:1175–1183. [PubMed: 21712086]
6. Dhar SK, Xu Y, St. Clair DK. Nuclear factor kB- and specificity protein 1 - dependent p53 mediated bi-directional regulation of the human manganese superoxide dismutase gene. J Biological Chem. 2010; 285:9835–9846.
7. Cho H-Y, Reddy SPM, Yamamoto M, Kleeberger SR. The transcription factor Nrf2 protects against pulmonary fibrosis. FASEB J. 2004; 18:1258–1260. [PubMed: 15208274]
8. Reddy NM, Potteti HR, Mariani TJ, Biswal S, Reddy SP. Conditional deletion of Nrf2 in airway epithelium exacerbates acute lung injury and impairs the resolution of inflammation. Am J Respir Cell Mol Biol. 2011; 45:1161–1168. [PubMed: 21659655]
9. Kim SB, Pandita RK, Eskiocak U, Ly P, Kaisani A, Kumar R, Cornelius C, Wright WE, Pandita TK, Shay JW. Targeting of Nrf2 induces DNA damage signaling and protects colonic epithelial cells from ionizing radiation. Proc Natl Acad Sci USA. 2012; 109:E2949–E2955. [PubMed: 23045680]

10. Rajagopalan MS, Stone B, Rwigema J-C, Salimi U, Epperly MW, Goff J, Franicola D, Dixon T, Cao S, Zhang X, Buchholz BM, Bauer AJ, Choi S, Bakkenist C, Wang H, Greenberger JS. Intraesophageal manganese superoxide dismutase-plasmid liposomes ameliorates novel total-body and thoracic radiation sensitivity of *Nos1* $^{-/-}$ mice. Radiat Res. 2010; 174:297–312. [PubMed: 20726721]
11. Rwigema J-CM, Beck B, Wang W, Doemling A, Epperly MW, Shields D, Goff JP, Franicola D, Dixon T, Frantz M-C, Wipf P, Tyurina Y, Kagan VE, Wang H, Greenberger JS. Two strategies for the development of mitochondrion-targeted small molecule radiation damage mitigators. Int J Radiat Oncol Biol Phys. 2011; 80:860–868. [PubMed: 21493014]
12. Goff JP, Epperly MW, Shields D, Wipf P, Dixon T, Greenberger JS. Radiobiologic effects of GS-nitroxide (JP4-039) in the hematopoietic syndrome. In Vivo. 2011; 25:315–324. [PubMed: 21576404]
13. Greenberger JS. Sensitivity of corticosteroid-dependent, insulin-resistant lipogenesis in marrow preadipocytes of mutation diabetic-obese mice. Nature. 1978; 275:752–754. [PubMed: 703842]
14. Sakakeeny MA, Greenberger JS. Granulopoiesis longevity in continuous bone marrow cultures and factor dependent cell line generation: Significant variation among 28 inbred mouse strains and outbred stocks. J Nat Canc Inst. 1982; 68:305–317.
15. Greenberger JS, Sakakeeny MA, Humphries KC, Eaves CG, Eckner RJ. Demonstration of permanent factor-dependent multipotential (erythroid/neutrophil/basophil) hematopoietic progenitor cell lines. Proc Natl Acad Sci USA. 1983; 80:2931–2935. [PubMed: 6574462]
16. Greenberger JS, Sakakeeny MA, Davis LM, Moloney WC, Reid D. Biologic properties of factor independent nonadherent hematopoietic and adherent pre adipocyte cell lines derived from continuous bone marrow cultures. Leukemia Res. 1984; 8:363–375. [PubMed: 6431199]
17. Epperly MW, Cao S, Zhang X, Franicola D, Kanai AJ, Greenberger EE, Greenberger JS. Increased longevity of hematopoiesis in continuous bone marrow cultures derived from *mtNos* $^{-/-}$ homozygous recombinant negative mice correlates with increased radioresistance of hematopoietic and bone marrow stromal cells. Exp Hemat. 2007; 35:137–145. [PubMed: 17198882]
18. Epperly MW, Cao S, Goff J, Shields D, Zhou S, Glowacki J, Greenberger JS. Increased longevity of hematopoiesis in continuous bone marrow cultures and adipocytogenesis in marrow stromal cells derived from Smad3 $^{-/-}$ mice. Exp Hemat. 2005; 33:353–362. [PubMed: 15730859]
19. O'Sullivan R, Goff J, Shields D, Epperly M, Greenberger JS, Glowacki J. Cell biologic parameters of accelerated osteoporosis in SAMP6 mice are demonstrated in long-term bone marrow culture senescence and in the biology of bone marrow stromal cell lines. Exp Hemat. 2012; 40:499–509. [PubMed: 22326715]
20. Epperly MW, Sikora C, Defilippi S, Gretton J, Zhan Q, Kufe DW, Greenberger JS. MnSOD inhibits irradiation-induced apoptosis by stabilization of the mitochondrial membrane against the effects of SAP kinases p38 and JNK1 translocation. Radiat Res. 2002; 157:568–577. [PubMed: 11966323]
21. Epperly MW, Gretton JE, Bernarding M, Nie S, Rasul B, Greenberger JS. Mitochondrial localization of copper/zinc superoxide dismutase (CuZnSOD) confers radioprotective functions *in vitro* and *in vivo*. Radiat Res. 2003; 160:568–578. [PubMed: 14565825]
22. Epperly MW, Osipov AN, Martin I, Kawai K, Borisenko GG, Jefferson M, Bernarding M, Greenberger JS, Kagan VE. Ascorbate as a redox-sensor and protector against irradiation-induced oxidative stress in 32D cl 3 hematopoietic cells and subclones overexpressing human manganese superoxide dismutase. Int J Radiat Oncol Biol Phys. 2004; 58:851–861. [PubMed: 14967442]
23. Bernard ME, Kim H, Berhane H, Epperly MW, Franicola D, Zhang X, Houghton F, Shields D, Wang H, Bakkenist CJ, Frantz M-C, Wipf P, Greenberger JS. GS-nitroxide (JP4-039) mediated radioprotection of human Fanconi anemia cell lines. Radiat Res. 2011; 176:603–612. [PubMed: 21939290]
24. Shelton P, Jaiswal AK. The transcription factor NF-E2-related factor 2 (Nrf2): A proto-oncogene? FASEB J. 2013; 27:414–423. [PubMed: 23109674]
25. Lechpammer S, Epperly MW, Zhou S, Nie S, Glowacki J, Greenberger JS. Antioxidant pool regulated adipocyte differentiation *Sod2* $^{-/-}$ bone marrow stromal cells. Exp Hemat. 2005; 33:1201–1208. [PubMed: 16219542]

26. Mauch P, Greenberger JS, Botnick LE, Hannon EC, Hellman S. Evidence for structured variation in self-renewal capacity within long-term bone marrow cultures. Proc Natl Acad Sci USA. 1980; 77:2927–2930. [PubMed: 6930675]

27. Neben S, Anklesaria P, Greenberger JS, Mauch P. Quantitation of murine hematopoietic stem cells *in vitro* by limiting dilution analysis of cobblestone area formation on a clonal stromal cell line. Exp Hematol. 1993; 21:438–444. [PubMed: 8440341]

28. Tsai JJ, Dudakov JA, Takahashi K, Shieh J-H, Verlardi E, Holland AM, Singer NV, West ML, Smith OM, Young LF, Shono Y, Ghosh A, Hanash AM, Tran HT, Moore MAS, van den Brink MRM. Nrf2 regulates haematopoietic stem cell function. Nat Cell Biol. 2013; 15:309–315. [PubMed: 23434824]

29. Epperly MW, Chaillet JR, Kalash R, Shaffer B, Goff J, Shields D, Dixon T, Wang H, Berhane H, Kim J-H, Greenberger JS. Conditional radioresistance of tet-inducible manganese superoxide dismutase bone marrow stromal cells. Radiat Res. in press.

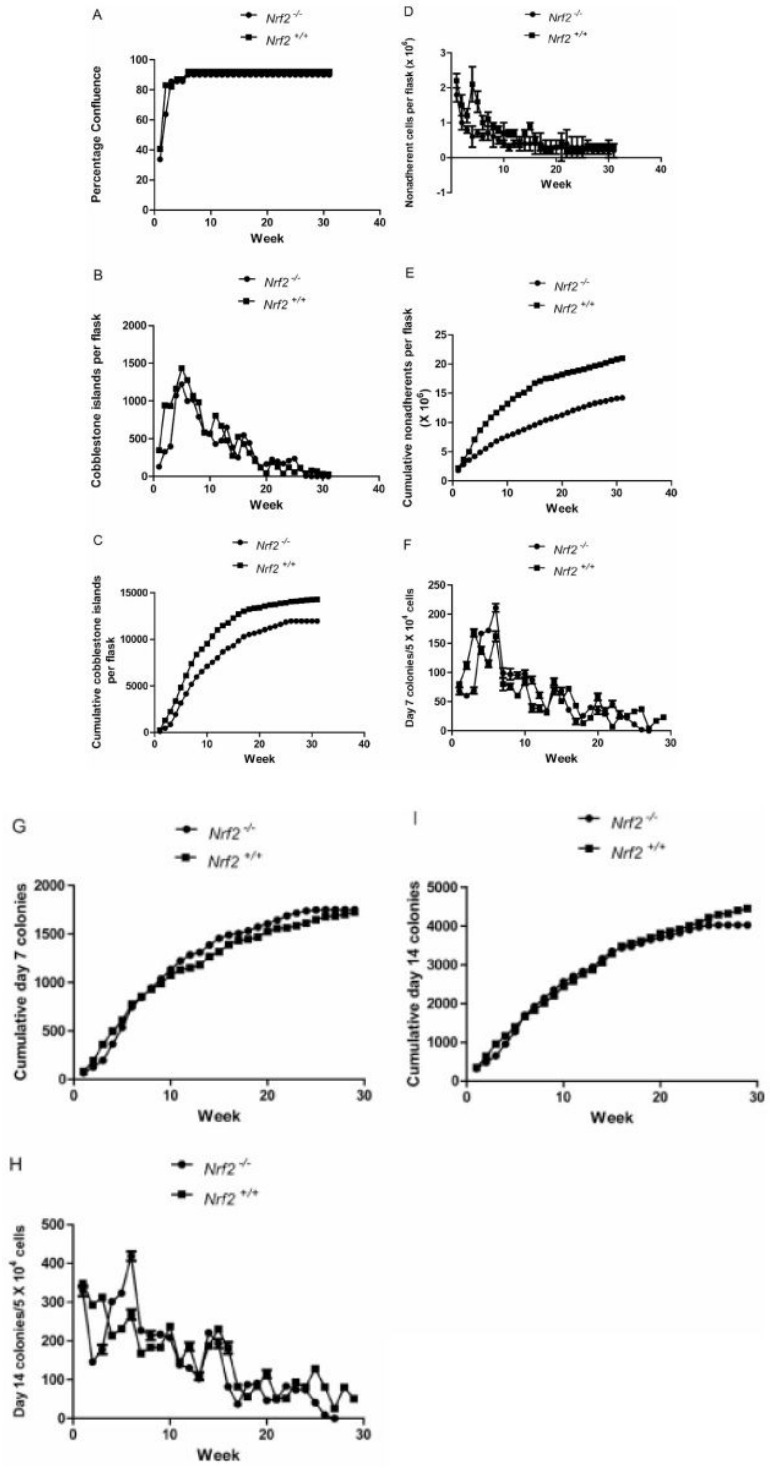

Figure 1.

Hematopoiesis longevity in long-term cultures of marrow from Nrf2$^{-/-}$ mice. A: percentage confluence; B: healthy cobblestone islands; C: cumulative cobblestone islands; D: weekly nonadherent cells; E: cumulative nonadherent cells; F: weekly day 7 colony-forming

progenitor cells; G: cumulative day 7 colony-forming progenitor cells; H: weekly day 14 colony-forming progenitor cells; and I: cumulative day 14 colony-forming progenitor cells.

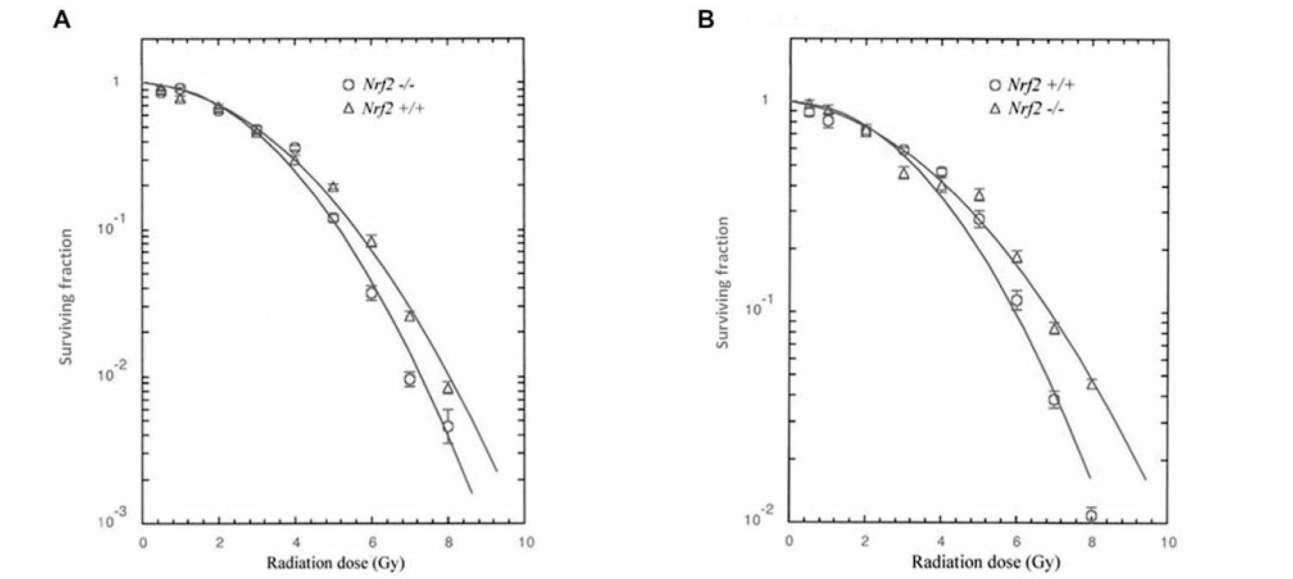

Cell line	D_0 (Gy)	ñ	Plating efficiency
Nrf2 $^{+/+}$	1.10 ± 0.13	3.25 ± 0.25	52.6 ± 8.6
Nrf2 $^{-/-}$	1.54 ± 0.13 (p=0.0696)	7.85 ± 0.84 (p=0.0255)	37.0 ± 9.2 (p=0.2641)

Cell line	D_0 (Gy)	ñ	Plating efficiency
Nrf2 $^{+/+}$	1.23 ± 0.03	1.16 ± 0.15	52.8 ± 9.3
Nrf2 $^{-/-}$	2.17 ± 0.13 (p=0.0031)	1.38 ± 0.38 (p=0.5790)	4.4 ± 2.3 (p=0.0330)

Figure 2.

Radiosensitivity of cell lines derived from long-term culture of marrow from ($Nrf2^{-/-}$) mice: bone marrow stromal (A) and Il-3 dependent cell lines. D_0 (slope of the linear portion of the survival curve), ñ (back extrapolation of the linear portion of the survival curve to the Y axis representing the width of the shoulder on the survival curve), and plating efficiency were calculated as described in the Materials and Methods and in (11).

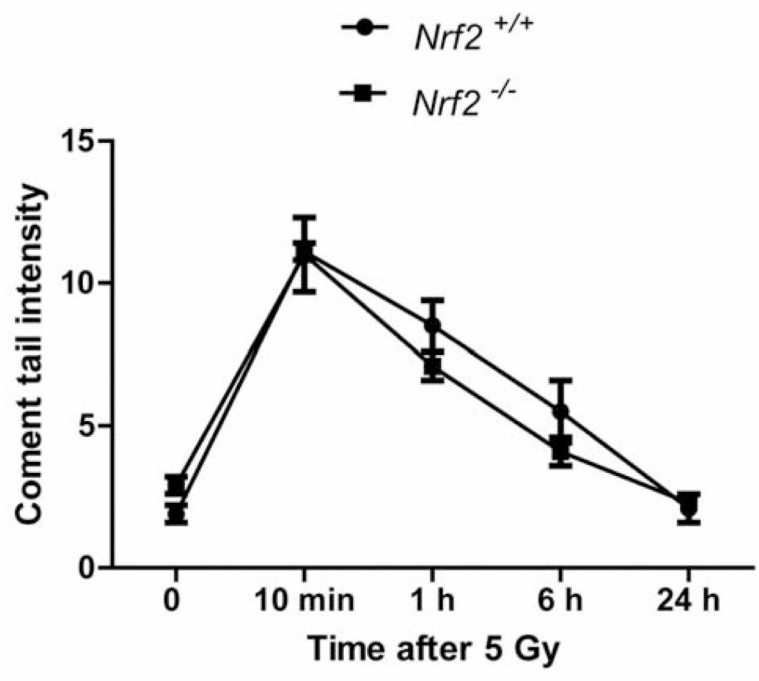

Figure 3.

DNA repair in Nrf2$^{-/-}$ compared to Nrf2$^{+/+}$ bone marrow stromal cells. DNA repair in irradiated stromal cell lines was quantitated using the comet assay according to published methods (29).

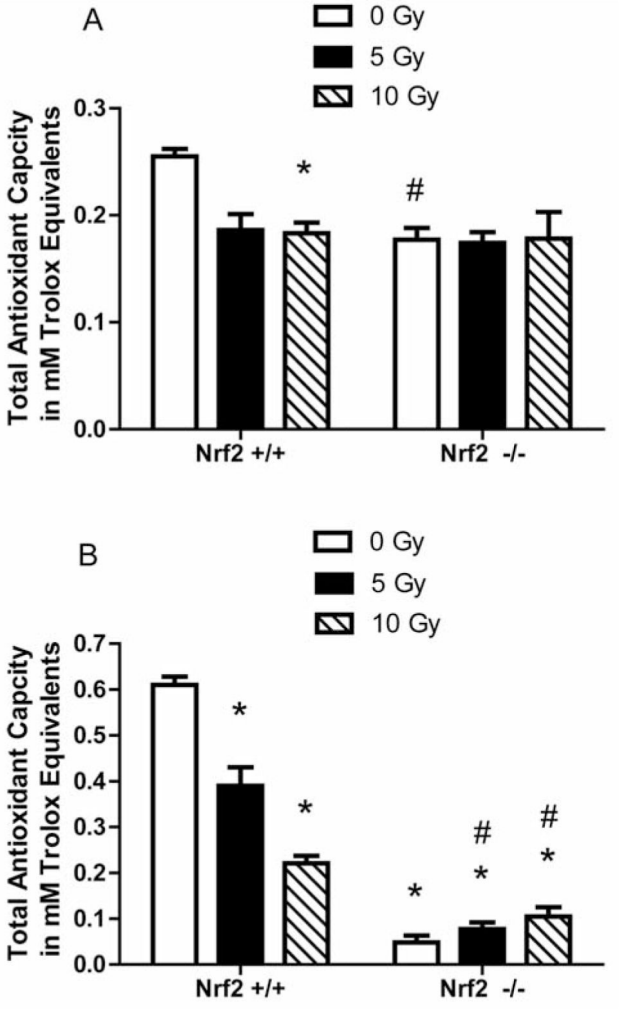

Figure 4.

Measurement of antioxidant stores in ($Nrf2^{-/-}$) marrow stromal and (Il-3) dependent hematopoietic cells 24 hours after 0, 5 Gy or 10 Gy irradiation. Marrow stromal cell lines (A) and IL-3 dependent hematopoietic progenitor cell lines (B) were assayed for antioxidant stores using the Trolox assay (29). Data is presented as total antioxidant capacity in mM trolox equivalents per 1 mg/ml of sample. For the marrow stromal cell lines (A), *p=0.0035 comparing $Nrf2^{+/+}$ cells 24 h after 10 Gy to $Nrf2^{+/+}$ cells while # has a p=0.0205 comparing nonirradiated $Nrf2^{-/-}$ cells to nonirradiated $Nrf2^{-/-}$ cells. In figure 4B, * has a $p<0.05$ compared to nonirradiated $Nrf2^{+/+}$ Il-3 dependent hematopoietic cells while # has a $p<0.015$ when compared to $Nrf2^{-/-}$ at 0 Gy.

Table I

Analysis of hematopoiesis in long-term marrow cultures of Nrf2$^{-/-}$ mice: weekly percent confluence of adherent cells

	Week 1	Week 2	Week 3	Week 4	Week 5
Nrf2 $^{-/-}$	33.8±2.5 (n=4)	63.8±3.2 (n=4)	85.6±1.2 (n=4)	85.6±1.2 (n=4)	85.6±1.2 (n=4)
Nrf2 $^{+/+}$	40.6±3.7 (n=4)	82.5±2.0 (n=4)	80.0±0.0 (n=4)	85.0±0.0 (n=4)	85.0±0.0 (n=4)
P	**0.0225**	**<0.0001**	**0.0001**	0.3910	0.3910
	Week 6	Week 7	Week 8	Week 9	Week 10
Nrf2 $^{-/-}$	90.0±0.0 (n=4)	90.0±0.0 (n=4)	90.0±0.0 (n=4)	90.0±0.0 (n=4)	90.0±0.0 (n=4)
Nrf2 $^{+/+}$	90.0±0.0 (n=4)	90.0±0.0 (n=3)	90.0±0.0 (n=3)	90.0±0.0 (n=3)	90.0±0.0 (n=2)
P	1	1	1	1	1
	Week 11	Week 12	Week 13	Week 14	Week 15
Nrf2 $^{-/-}$	90.0±0.0 (n=4)	90.0±0.0 (n=4)	90.0±0.0 (n=4)	90.0±0.0 (n=4)	90.0±0.0 (n=4)
Nrf2 $^{+/+}$	90.0±0.0 (n=2)	90.0±. (n=1)	90.0±. (n=1)	90.0±. (n=1)	90.0±. (n=1)
P	1	1	1	1	1
	Week 16	Week 17	Week18	Week 19	Week 20
Nrf2 $^{-/-}$	90.0±0.0 (n=4)	90.0±0.0 (n=4)	90.0±0.0 (n=4)	90.0±0.0 (n=4)	90.0±0.0 (n=4)
Nrf2 $^{+/+}$	90.0±. (n=1)	90.0±0.0 (n=1)	90.0±0.0 (n=1)	90.0±.0.0 (n=1)	90.0±0.0 (n=1)
P	1	1	1	1	1
	Week 21	Week 22	Week 23	Week 24	Week25
Nrf2 $^{-/-}$	90.0±0.0 (n=4)	90.0±0.0 (n=4)	90.0±0.0 (n=4)	90.0±0.0 (n=4)	90.0±0.0 (n=4)
Nrf2 $^{+/+}$	90.0±0.0 (n=1)	90.0±0.0 (n=1)	90.0±0.0 (n=1)	90.0±0.0 (n=1)	90.0±0.0 (n=1)
P	1	1	1	1	1
	Week 26	Week 27	Week 28	Week 29	Week 30
Nrf2 $^{-/-}$	90.0±0.0 (n=4)				
Nrf2 $^{+/+}$	90.0±0.0 (n=1)				
P	1				

Data are summarized as mean±standard deviation, n is the number of mice used, and *p*-values were calculated with the two-sided two sample *t*-test. Significant *p*-values are shown in bold.

Table II

Analysis of hematopoiesis in long-term marrow cultures of Nrf2$^{-/-}$ mice: weekly cobblestone number

	Week 1	Week 2	Week 3	Week 4	Week 5
Nrf2 $^{-/-}$	129.5±53.4 (n=4)	327.0±101.3 (n=4)	398.3±152.8 (n=4)	1070.0±172.8 (n=4)	1220.5±202.5 (n=4)
Nrf2 $^{+/+}$	348.5±81.1 (n=4)	941.0±122.7 (n=4)	935.5±253.6 (n=4)	1161.8±200.6 (n=4)	1433.0±118.1 (n=4)
P	**0.0041**	**0.0002**	**0.0110**	0.5142	0.1198
	Week 6	Week 7	Week 8	Week 9	Week 10
Nrf2 $^{-/-}$	1001.0±157.2 (n=4)	1016.8±135.2 (n=4)	792.0±105.9 (n=4)	580.3±166.4 (n=4)	561.3±155.4 (n=4)
Nrf2 $^{+/+}$	1303.0±200.2 (n=4)	1042.3±207.6 (n=3)	969.3±166.6 (n=3)	557.0±162.2 (n=3)	567.5±238.3 (n=2)
P	0.0553	0.8498	0.1425	0.8607	0.9699
	Week 11	Week 12	Week 13	Week 14	Week 15
Nrf2 $^{-/-}$	431.0±181.3 (n=4)	415.5±219.8 (n=4)	680.5±246.3 (n=4)	399.8±135.0 (n=4)	250.3±58.3 (n=4)
Nrf2 $^{+/+}$	808.0±186.7 (n=2)	671.0±. (n=1)	478.5±. (n=1)	272.0±. (n=1)	525.0±. (n=1)
P	0.0757				
	Week 16	Week 17	Week18	Week 19	Week 20
Nrf2 $^{-/-}$	594.0±293.5 (n=4)	518.0±455.9 (n=4)	278.0±235.4 (n=4)	145.3±111.9 (n=4)	148.8±182.0 (n=4)
Nrf2 $^{+/+}$	429.0±. (n=1)	313.0±. (n=1)	206.0±. (n=1)	118.0±. (n=1)	44.0±. (n=1)
P					
	Week 21	Week 22	Week 23	Week 24	Week25
Nrf2 $^{-/-}$	200.8±238.5 (n=4)	176.8±220.8 (n=4)	150.3±205.1 (n=4)	184.3±318.8 (n=4)	205.8±395.0 (n=4)
Nrf2 $^{+/+}$	189.0±. (n=1)	127.0±. (n=1)	38.0±. (n=1)	120.0±. (n=1)	55.0±. (n=1)
P					
	Week 26	Week 27	Week 28	Week 29	Week 30
Nrf2 $^{-/-}$	93.0±158.0 (n=4)				
Nrf2 $^{+/+}$	118.0±. (n=1)				
P					

Data are summarized as mean±standard deviation, n is the number of mice used, and *p*-values were calculated with the two-sided two sample *t*-test. Significant *p*-values are shown in bold.

Table III

Analysis of hematopoiesis in long-term marrow cultures from Nrf2$^{-/-}$ mice: weekly non-adherent cell number

	Week 1	Week 2	Week 3	Week 4	Week 5
Nrf2 $^{-/-}$	17.81±1.55 (n=4)	9.97±1.55 (n=4)	8.08±0.31 (n=4)	6.32±1.54 (n=4)	6.98±0.82 (n=4)
Nrf2 $^{+/+}$	22.22±1.28 (n=4)	15.15±1.47 (n=4)	12.44±1.60 (n=4)	21.27±4.36 (n=4)	16.34±2.55 (n=4)
P	**0.0047**	**0.0028**	**0.0106**	**0.0007**	**0.0004**
	Week 6	Week 7	Week 8	Week 9	Week 10
Nrf2 $^{-/-}$	6.01±0.89 (n=4)	6.91±1.16 (n=4)	5.91±1.48 (n=4)	4.80±1.38 (n=4)	1.87±2.24 (n=4)
Nrf2 $^{+/+}$	9.92±1.86 (n=4)	10.61±1.42 (n=3)	8.45±0.82 (n=3)	8.10±0.65 (n=3)	7.15±2.89 (n=2)
P	**0.0090**	**0.0124**	**0.0452**	**0.0128**	0.0655
	Week 11	Week 12	Week 13	Week 14	Week 15
Nrf2 $^{-/-}$	3.09±0.37 (n=4)	3.84±1.31 (n=4)	3.79±2.19 (n=4)	3.99±1.44 (n=4)	3.84±1.01 (n=4)
Nrf2 $^{+/+}$	7.51±0.81 (n=2)	7.34±. (n=1)	4.13±. (n=1)	6.60±. (n=1)	8.57±. (n=1)
P	**0.0006**				
	Week 16	Week 17	Week18	Week 19	Week 20
Nrf2 $^{-/-}$	4.15±1.43 (n=4)	4.36±1.85 (n=4)	3.41±1.35 (n=4)	2.66±1.13 (n=4)	2.78±1.67 (n=4)
Nrf2 $^{+/+}$	4.73±. (n=1)	3.14±. (n=1)	1.89±. (n=1)	2.37±. (n=1)	2.90±. (n=1)
P					
	Week 21	Week 22	Week 23	Week 24	Week25
Nrf2 $^{-/-}$	3.35±2.54 (n=4)	3.71±2.90 (n=4)	3.16±1.79 (n=4)	3.09±2.67 (n=4)	2.81±2.47 (n=4)
Nrf2 $^{+/+}$	3.57±. (n=1)	2.04±. (n=1)	2.05±. (n=1)	2.05±. (n=1)	2.46±. (n=1)
P					
	Week 26	Week 27	Week 28	Week 29	Week 30
Nrf2 $^{-/-}$	2.70±1.76 (n=4)				
Nrf2 $^{+/+}$	2.77±. (n=1)				
P					

Data are summarized as mean±standard deviation, n is the number of mice used, and *p*-values were calculated with the two-sided two sample *t*-test. Significant *p*-values are shown in bold. (×100000).

Table IV

Analysis of hematopoiesis in long-term marrow cultures from Nrf2$^{-/-}$ mice: day 7 colony forming progenitor cell counts

	Week 1	Week 2	Week 3	Week 4	Week 5
Nrf2 $^{-/-}$	68.0±6.0 (n=3)	59.7±3.5 (n=3)	68.7±5.5 (n=3)	167.3±4.7 (n=3)	172.0±4.0 (n=3)
Nrf2 $^{+/+}$	80.3±4.0 (n=3)	112.3±6.5 (n=3)	167.7±6.5 (n=3)	137.7±6.5 (n=3)	114.7±6.0 (n=3)
P	**0.0418**	**0.0002**	**<0.0001**	**0.0031**	**0.0002**
	Week 6	Week 7	Week 8	Week 9	Week 10
Nrf2 $^{-/-}$	211.0±7.0 (n=3)	98.7±8.6 (n=3)	97.0±9.6 (n=3)	95.3±5.5 (n=3)	98.3±6.0 (n=3)
Nrf2 $^{+/+}$	162.0±9.0 (n=3)	79.7±11.0 (n=3)	75.7±5.1 (n=3)	60.0±2.0 (n=3)	83.7±6.0 (n=3)
P	**0.0017**	0.0778	**0.0277**	**0.0005**	**0.0407**
	Week 11	Week 12	Week 13	Week 14	Week 15
Nrf2 $^{-/-}$	86.7±6.5 (n=3)	61.0±5.0 (n=3)	34.3±4.5 (n=3)	68.0±6.0 (n=3)	68.3±6.0 (n=3)
Nrf2 $^{+/+}$	39.0±7.0 (n=3)	38.3±6.0 (n=3)	31.3±4.5 (n=3)	84.0±6.0 (n=3)	51.3±4.5 (n=3)
P	**0.0010**	**0.0074**	0.4609	**0.0309**	**0.0174**
	Week 16	Week 17	Week18	Week 19	Week 20
Nrf2 $^{-/-}$	35.7±4.0 (n=3)	16.0±5.0 (n=3)	26.3±4.5 (n=3)	40.0±3.6 (n=3)	35.3±6.5 (n=3)
Nrf2 $^{+/+}$	72.3±2.5 (n=3)	43.0±4.0 (n=3)	13.0±3.6 (n=3)	21.7±4.5 (n=3)	58.0±6.0 (n=3)
P	**0.0002**	**0.0019**	**0.0161**	**0.0053**	**0.0114**
	Week 21	Week 22	Week 23	Week 24	Week25
Nrf2 $^{-/-}$	34.3±5.0 (n=3)	45.7±5.5 (n=3)	28.0±6.0 (n=3)	22.0±3.6 (n=3)	10.7±2.5 (n=3)
Nrf2 $^{+/+}$	29.3±4.2 (n=3)	7.0±1.0 (n=3)	24.0±4.0 (n=3)	25.7±3.5 (n=3)	33.0±3.0 (n=3)
P	0.2555	**0.0003**	0.3911	0.2756	**0.0006**

Data are summarized as mean±standard deviation, n is the number of observations, and *p*-values were calculated with the two-sided two sample *t*-test. Significant *p*-values are shown in bold. (5×10^4 cells/ml).

Table V

Analysis of hematopoiesis in long-term marrow cultures from Nrf2$^{-/-}$ mice: day 14 colony forming progenitor cell counts

	Week 1	Week 2	Week 3	Week 4	Week 5
Nrf2 $^{-/-}$	329.0±13.7 (n=3)	146.7±8.6 (n=3)	177.7±11.9 (n=3)	300.7±6.5 (n=3)	323.3±6.5 (n=3)
Nrf2 $^{+/+}$	354.7±13.5 (n=3)	288.7±9.3 (n=3)	303.0±14.9 (n=3)	204.7±16.3 (n=3)	222.0±15.9 (n=3)
P	0.0823	**<0.0001**	**0.0003**	**0.0007**	**0.0005**
	Week 6	Week 7	Week 8	Week 9	Week 10
Nrf2 $^{-/-}$	419.3±12.1 (n=3)	227.3±6.5 (n=3)	214.3±11.9 (n=3)	217.0±8.2 (n=3)	208.3±7.0 (n=3)
Nrf2 $^{+/+}$	275.3±16.6 (n=3)	172.0±8.0 (n=3)	186.3±8.0 (n=3)	179.7±6.5 (n=3)	240.3±8.6 (n=3)
P	**0.0003**	**0.0007**	**0.0280**	**0.0035**	**0.0076**
	Week 11	Week 12	Week 13	Week 14	Week 15
Nrf2 $^{-/-}$	138.0±6.0 (n=3)	129.7±4.0 (n=3)	103.0±9.2 (n=3)	221.3±7.0 (n=3)	193.0±12.1 (n=3)
Nrf2 $^{+/+}$	146.0±6.0 (n=3)	177.0±15.0 (n=3)	114.0±11.1 (n=3)	192.7±10.6 (n=3)	224.7±11.0 (n=3)
P	0.1778	**0.0062**	0.2570	**0.0175**	**0.0286**
	Week 16	Week 17	Week18	Week 19	Week 20
Nrf2 $^{-/-}$	82.0±5.6 (n=3)	37.0±4.6 (n=3)	87.3±6.1 (n=3)	90.0±6.0 (n=3)	47.0±4.6 (n=3)
Nrf2 $^{+/+}$	182.3±10.6 (n=3)	84.7±6.0 (n=3)	58.3±6.0 (n=3)	86.7±7.0 (n=3)	109.7±10.0 (n=3)
P	**0.0001**	**0.0004**	**0.0043**	0.5659	**0.0006**
	Week 21	Week 22	Week 23	Week 24	Week25
Nrf2 $^{-/-}$	48.7±3.2 (n=3)	83.0±5.6 (n=3)	74.0±4.0 (n=3)	74.3±5.5 (n=3)	
Nrf2 $^{+/+}$	50.0±4.0 (n=3)	48.7±6.5 (n=3)	95.0±4.0 (n=3)	84.0±6.0 (n=3)	
P	0.6760	**0.0023**	0.0030	**0.1090**	

Data are summarized as mean±standard deviation, n is the number of observations, and *p*-values were calculated with the two-sided two sample *t*-test. Significant *p*-values are shown in bold.